Coral hosts actively accumulate inorganic carbon for zooxanthellae to maintain symbiotic relationships

Boya Zhang[1], Si Tang[1], Lu Liu[1], Meiting Xu[2], Yaqing Liu[1], Jianming Zhu[1], Weimin Xiao[3], Hongsheng Bi[4], Jin Zhou[1], Mark C. Benfield[5] & Zhonghua Cai[1,6,*]

[1]Shenzhen Public Platform for Screening and Application of Marine Microbial Resources, Tsinghua Shenzhen International Graduate School, Shenzhen 518055 Guangdong Province, PR China.

[2]School of Environment, Harbin Institute of Technology, Harbin 150090 Heilongjiang Province, PR China.

[3]Shenzhen Academy of Metrology and Quality Inspection, Shenzhen 518109 Guangdong Province, PR China.

[4]Chesapeake Biological Laboratory, University of Maryland Center for Environmental Science, Solomons, MD, USA.

[5]College of the Coast and Environment Department of Oceanography and Coastal Sciences, Louisiana State University, Baton Rouge, LA 70803, USA.

[6]Technology Innovation Center for Marine Ecology and Human Factor Assessment of Natural Resources Ministry, Tsinghua Shenzhen International Graduate School, Shenzhen 518055 Guangdong Province, PR China.

[*]Corresponding author: Zhonghua Cai (caizh@sz.tsinghua.edu.cn)

Abstract

High primary productivity of coral reefs is widely attributed to the mutualistic symbiosis between corals and zooxanthellae. The mechanisms that maintain this symbiosis remain poorly explored. Given the high carbon demands by zooxanthellae, we hypothesized that corals may have evolved strategies to actively accumulate dissolved inorganic carbon (DIC) to maintain the host-algae symbiosis. Carbon supplies and consumption were evaluated in the scleractinian coral (*Goniopora lobata*) and zooxanthellae under light and dark conditions. Results suggest that zooxanthellae are high DIC consumers, requiring about 2-3 fold more DIC than free-living species. The corals were high DIC producers, but were unable to effectively eliminate all the DIC they produced and actively accumulated DIC in the light, with concentrations up to 4.2 fold higher than in the surrounding seawater. Transcriptomic analysis found several DIC enrichment pathways, including CO_2 concentrating mechanisms, respiration, calcification and phosphoenolpyruvate carboxylase. It appears that corals actively enrich DIC for zooxanthellae.

35 **Introduction**

36 Coral reefs are recognized as having the highest levels of primary productivity
37 (1500-5000 gC $m^{-2}a^{-1}$) in nature[1], while growing in shallow oligotrophic waters[2,3]. The
38 high productivity of coral reefs is widely attributed to their symbiotic relationship with
39 the microalgal zooxanthellae[4,5,6].

40 Within this mutualistic relationship, it is believed that coral provides living space for
41 zooxanthellae, as well as some nutrients such as ammonia, urea, and
42 polyphosphates[7,8,9]. In return, the symbiont algae transfer more than 90% of their
43 photosynthesis to the coral host with organic products such as glucose, glycerol,
44 amino acids and lipids[10,11,12]. A more detailed understanding of how the symbiosis is
45 initiated and maintained remains poorly understood.

46 From a stoichiometric perspective, high productivity requires a high carbon supply,
47 and providing the CO_2 to symbiotic zooxanthellae is potentially a challenge for corals
48 for three reasons: (1) CO_2 diffuses 10,000 times more slowly in water than in air[13]; (2)
49 the low CO_2 affinity of microalgal Rubisco (the type II Rubisco of zooxanthellae
50 possesses an even lower CO_2 affinity[14,15]); and (3) symbiotic microalgae within the
51 coral tissue are physically separated from dissolved inorganic carbon (DIC, including
52 CO_2, HCO_3^-, CO_3^{2-} and H_2CO_3 etc.) in the surrounding seawater. However, based on
53 their success as a whole, one could logically presume that DIC concentrations inside
54 corals should at least equal or even exceed ambient levels. In addition, the supply of
55 DIC to the symbionts and elimination between coral and symbionts should keep
56 balance, otherwise, the microalgal photosynthesis may be stressed by low DIC, and

this symbiosis may no longer function optimally.

Understanding the DIC metabolism of corals is quite challenging because the DIC within coral tissue is involved in several processes: (1) CO_2 generation by the respiration of coral and zooxanthellae; (2) CO_2 consumption for microalgal photosynthesis; and (3) HCO_3^- consumption and CO_2 generation due to coral calcification. Generally, coral respiration is deemed to be the major contributor of CO_2, but the fate of CO_2 remains contentious due to coral calcification[16]. Some suggest that CO_2 from host respiration will be actively consumed via symbiont photosynthesis [17]. Others argue that CO_2 will be rapidly transformed into HCO_3^- and used by the host itself for calcification to produce the $CaCO_3$ skeletons that are the structural basis of coral reefs[18]. Moreover, there is competition for HCO_3^- in seawater between coral calcification and microalgal photosynthesis[19,20,21], but some views hold that these two DIC consumption pathways are non-competitive[22,23,24], and that calcification can even contribute CO_2 required by photosynthesis. In addition, it is suggested that the heterotrophic feeding of coral hosts also affects symbionts, especially in light-limited deep water[25,26]. More research is needed to address these hypotheses.

Here, we explore the coral-algae symbiotic relationship based on the carbon supplies to the symbiotic system, and propose that coral hosts may actively accumulate DIC for high CO_2-demanding zooxanthellae. To test this hypothesis, the scleractinian coral (*Goniopora lobata*) was employed as a model. Various carbon source (HCO_3^- or glucose) utilization experiments were conducted under light or dark regimes to determine the carbon consumption characteristics of the coral hosts and

79 zooxanthellae symbionts, respectively. Finally, a CO_2 enrichment experiment was
80 performed to simulate the impact of high external DIC concentrations on coral
81 symbiosis.

82 **Results**

83 **Zooxanthellae DIC requirement**

84 To determine the photosynthetic DIC requirements of the symbiotic microalgae, the
85 specific growth rates and carbon consumption rates of a zooxanthellae monoculture
86 were evaluated at various dosages of $NaHCO_3$. In general, zooxanthellae grew faster
87 at higher DIC concentrations. The highest cell growth rate reached 0.53 d^{-1} at 8 mM
88 $NaHCO_3$, which is 2.08 and 1.34 times higher than that of cells grown with 2 mM and
89 4 mM $NaHCO_3$, respectively (Fig. 1a, Two-way ANOVA, $F_{2,6} = 3.427$, $p < 0.05$). As
90 expected, faster-growing cells consumed more DIC. The average DIC consumption
91 rates were 0.10 mM d^{-1}, 0.18 mM d^{-1}, and 0.26 mM d^{-1} corresponding to the 2 mM, 4
92 mM, and 8 mM $NaHCO_3$ treatments, respectively (Fig. 1b). In contrast, the DIC
93 concentration was almost constant in the control group (Fig. S1). It was noteworthy
94 that zooxanthellae grown with different $NaHCO_3$ concentrations all showed a linear
95 increase in biomass with DIC consumption, suggesting that external DIC
96 concentration is one of the limiting factors for its growth. Meanwhile, based on the
97 slope of linear regression (0.012 mol g^{-1}, Fig. 1b), it can be calculated that
98 zooxanthellae consume approximately 0.528 g of CO_2 per gram of biomass growth,
99 significantly higher than other free-living microalgae[27,28,29]. Evidently, natural seawater
100 with a DIC concentration around 3 mM is a carbon-deficient environment for

zooxanthellae, so whether the DIC concentration inside coral tissues is sufficiently high and how this is achieved merits investigation.

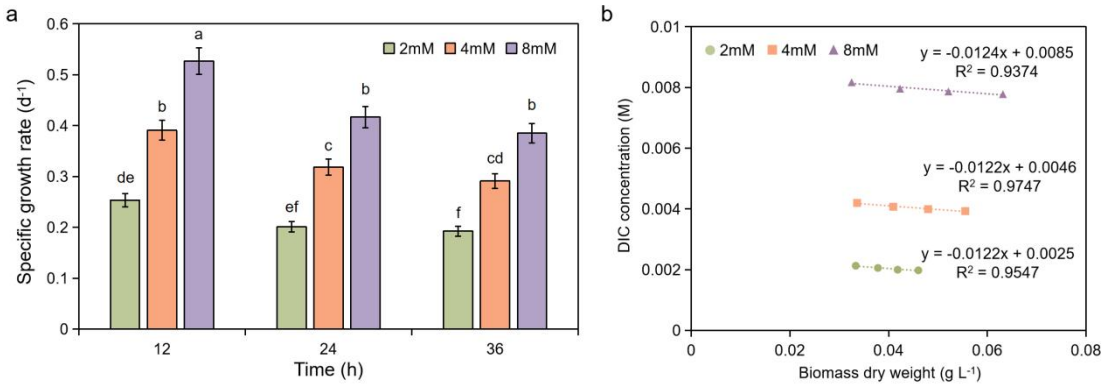

Fig. 1: Specific growth rate and carbon consumption analysis of monocultured zooxanthellae at different carbon concentrations. a, Specific growth rate of zooxanthellae at different stages. The graphs show the mean ± SD (n = 3). Letters above bars indicate a significant differences at $p < 0.05$. **b**, Relationship between carbon consumption and biomass growth of zooxanthellae (n = 3). Slopes indicate the carbon consumption for per gram of biomass growth of zooxanthellae. Data points are fitted with exponential decay functions. R^2 values indicating the goodness of fits are shown.

High DIC releases from corals require symbiont photosynthetic uptake

To investigate the carbon budget within the symbionic coral-zooxanthellae system, carbon supplies (organic (glucose) or inorganic ($NaHCO_3$)) experiments were performed under different light regimes. We first recorded the morphological responses of corals. As shown in Fig. 2a, when glucose was the only carbon source, the tentacles of the corals were obviously elongated in the light group (LG) compared with the dark group (DG). This morphological distinction in corals was also evident in

119 $NaHCO_3$, in which the coral remained healthy in the light group (LS) during 8 days,
120 while becoming lifelessness under dark conditions (DS). These results indicated that
121 the coral carbon utilization was influenced by the symbionts. Moreover, corals in the
122 DG still had tentacles protruding outward at day 8 compared with DS, while those in
123 the LG gradually shrank from day 4 compared with the LS. Theoretically, even though
124 glucose is not a preferred carbon source for zooxanthellae photosynthesis (LG vs LS),
125 as a nutrient that can be ingested by the host (DG vs DS), its supply in the dark should
126 have enabled the coral to grow normally. The question remains, why wasn't coral
127 growth healthy in the dark (DG vs LG)?
128 To further explain the reasons for the corals' morphological differences, we quantified
129 the changes in DIC and glucose concentrations in the external seawater and the coral
130 internal-tissues across all treatments. Although the corals grown with glucose can
131 consume glucose, we found that they cannot utilize glucose continuously after day 4
132 under dark conditions (from 0.1038 g L^{-1} to 0.0634 g L^{-1}, Fig. 2c), but were able to
133 continue glucose uptake in the presence of light (from 0.1027 g L^{-1} to 0.0304 g L^{-1}, Fig.
134 2c). Furthermore, we found that the utilization of external glucose was accompanied
135 by the accumulation of glucose and DIC in coral tissues (Fig. 2d,e). After the DG
136 group stopped taking up external glucose from day 4, the internal-tissue glucose
137 concentration stopped changing (0.0575 g L^{-1}), and the DIC concentration remained
138 stable after reaching a maximum (0.6009 g L^{-1}). While in LG group, the internal-tissue
139 glucose concentration kept increasing (from 0.0907 g L^{-1} to 0.1023 g L^{-1}), and the DIC
140 concentration gradually decreased (from 0.5632 g L^{-1} to 0.4297 g L^{-1}). These results

provided a good explanation for the morphological differences between corals in the LG and LS treatments: that corals could continuously utilize glucose in the light due to the consumption of internal-DIC by the symbiotic algae, whereas in the darkness, corals could not take up glucose when their internal-DIC reached a certain threshold. Unexpectedly, we detected significantly higher DIC concentrations inside coral tissues compared to external seawater. Under natural conditions (LS), the DIC concentration in coral tissues increased continuously, reaching a maximum of 4.2 times that of seawater on day 4 (Fig. 2d). Similar patterns were also observed in all of the other three treatments, and even in the DS also accumulated DIC in the tissues (Fig. 2bd). We also found that the higher DIC within the coral tissues was not being released into seawater in the organic carbon groups (LG and DG), because the DIC concentration in external seawater remained stable (~0.02 g L^{-1}, Fig. 2b).

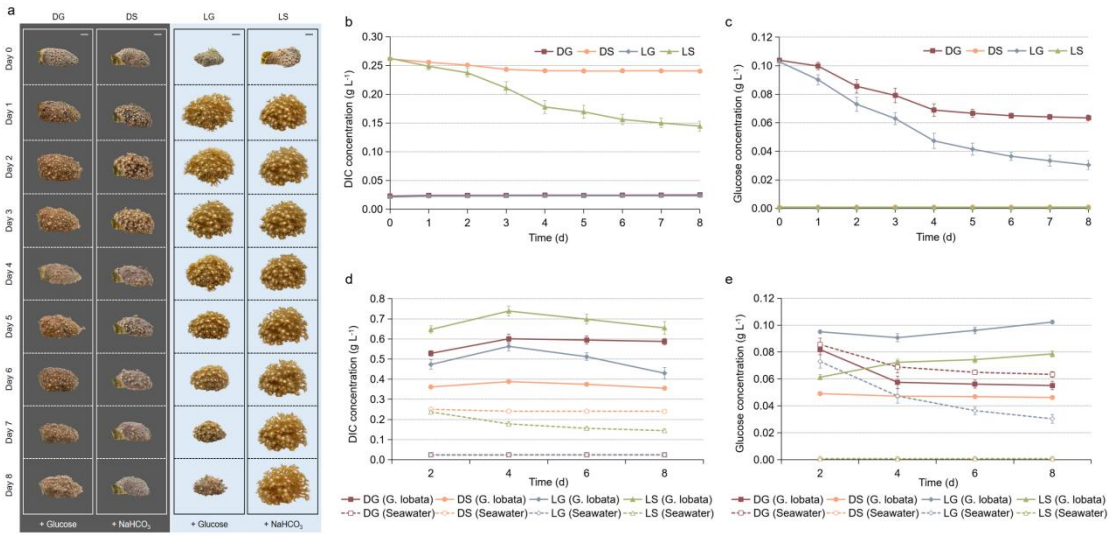

Fig. 2: Variation of coral morphology, DIC and glucose concentration in seawater and corals under different carbon sources and light conditions. a, Morphological changes of corals. Scale bars, 1 cm. **b**, DIC concentration in seawater. **c**, Glucose concentration in seawater. **d**, DIC concentration in corals. **e**, Glucose

concentration in corals. Straight lines and dotted lines indicate corals and seawater, respectively. The graphs show the mean ± SD (n = 3). DG indicates continuous darkness and glucose as the only carbon source. DS indicates continuous darkness and $NaHCO_3$ as the only carbon source. LG indicates light/dark = 12 h/12 h and glucose as the only carbon source. LS indicates light/dark = 12 h/12 h and $NaHCO_3$ as the only carbon source.

Enzymatic activities and gene expression in carbon fixation

To resolve the origin of the high DIC pools in coral tissues, we analyzed the variance in the activity of carbon fixation enzymes of coral as a whole, and the differentially expressed genes (DEGs) of the host and zooxanthellae, respectively. Coral grown in natural seawater (LS) was used as the control.

Carbonic anhydrases (CAs), catalyze the interconversion of CO_2 and HCO_3^-, and indicators of CO_2 concentrating mechanisms (CCMs), were used to evaluate the DIC transformation of the coral symbiotic system. As to the enzymatic activity of CAs, compared to LS (42.16 U g^{-1} $prot^{-1}$), CAs activity was eventually lowered to less than 75% in two dark groups (DG = 27.31 U g^{-1} $prot^{-1}$, DS = 16.67 U g^{-1} $prot^{-1}$), while the LG added glucose gradually elevated to 34.03 U g^{-1} $prot^{-1}$ (Fig. 3a), showing that the CCMs of corals were affected by light. Subsequently, the expression of genes encoding different types of CAs was found in both coral hosts and zooxanthellae. CAs are generally divided into α, β, and γ categories, with only α-CA in animals and all three categories in higher plants, algae, and cyanobacteria[30,31]. Notably, seven α-CA genes were identified in coral hosts with extremely poor DIC exclusion capacity, and

180 the DEGs of CA compared to LS was down-regulated in both dark groups (DG and
181 DS), but up-regulated in the light group LG (Fig. 3d), indicating that the CCMs of coral
182 hosts are associated with zooxanthellae photosynthesis. Moreover, different CA
183 subtypes and locations in zooxanthellae may perform different functions. For example,
184 the α-CA located in the cytoplasm and the β-CA1 in the chloroplasts were also
185 up-regulated under light conditions (Fig. 3d), while the β-CA2 located in the cytoplasm
186 was up-regulated in the dark groups (Fig. 3d).
187 In addition, we also identified an interesting pattern on the phosphoenolpyruvate
188 carboxylase (PEPCase) and phosphoenolpyruvate carboxykinase (PEPCKase), two
189 key enzymes for the biochemical CCMs, i.e., C_4 and crassulacean acid
190 metabolism (CAM)[32]. PEPCase catalyses the conversion of phosphoenolpyruvate
191 (PEP) to oxaloacetate and releases a CO_2 around Rubisco in C_4/CAM plants or
192 supplements malate to the TCA cycle directly in all organisms[33]. PEPCKase catalyses
193 the reverse pathway of PEPCase, converting oxaloacetate to PEP, and also plays a
194 key role in gluconeogenesis[34].
195 In terms of enzymatic activities, compared to LS, PEPCase was lower in the two
196 glucose-added groups and higher in DS (Fig. 3b), while PEPCKase was more active
197 in all treatments (especially in the two dark groups) (Fig. 3c). We attempted to explain
198 the possible reasons by DEGs. Results showed that the PEPC genes were not found
199 in coral hosts (Fig. 3e). Moreover, microalgal PEPC was mainly annotated as CAM
200 types and highly expressed in DS. PEPCK genes in host and zooxanthellae were
201 generally up-regulated in the dark (Fig. 3e), which was consistent with the results of

202 PEPCKase activities (Fig. 3c), indicating that the limitation of photosynthesis would

203 have forced both host and symbiont to synthesise glucose themselves. Notably, three

204 sequences were up-regulated in coral hosts under light conditions, especially in LS

205 (Fig. 3e-LS in red Gene ID), which was consistent with changes in PEPCKase activity

206 at later stages (Fig. 3c-LS).

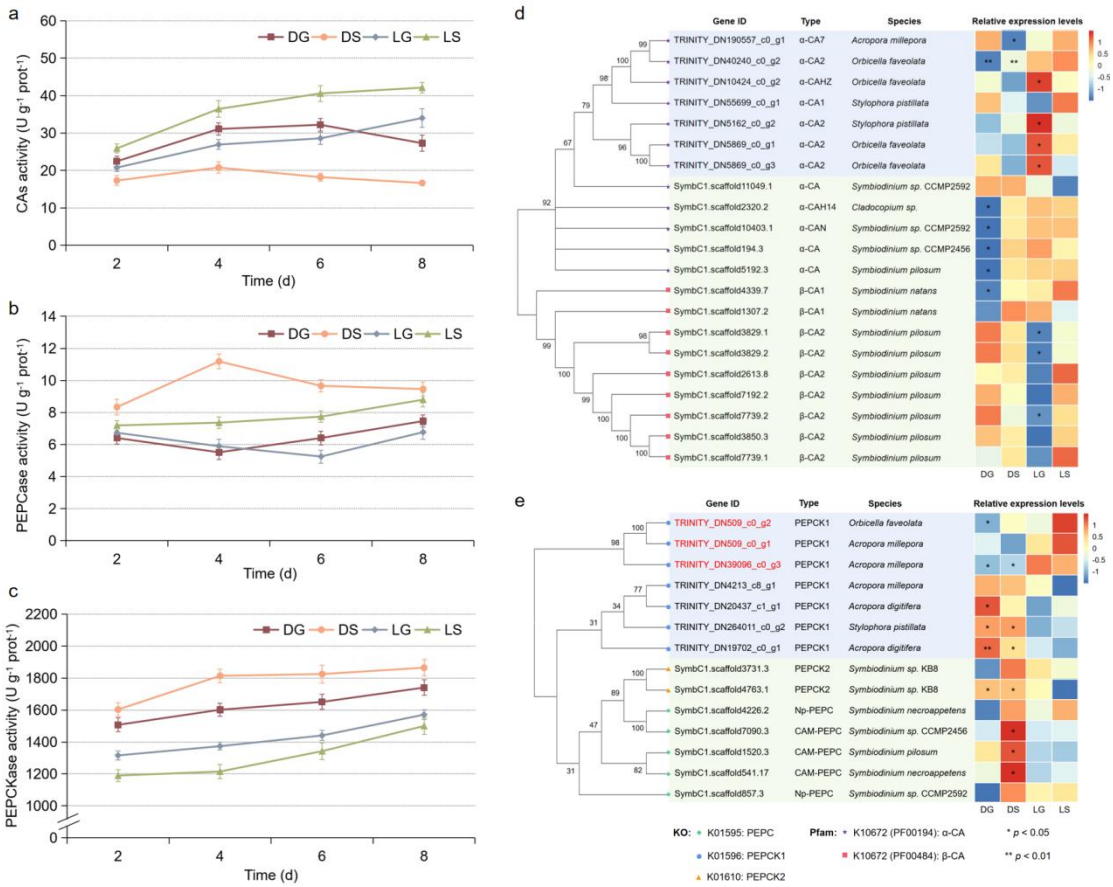

207

208 **Fig. 3: CAs, PEPCase and PEPCKase activities and gene expressions in coral**

209 **hosts and zooxanthellae. a**, CAs activity in corals. **b**, PEPCase activity in corals. **c**,

210 PEPCKase activity in corals. **d**, Differential expression of CA genes in coral hosts and

211 zooxanthellae. **e**, Differential expression of PEPC and PEPCK genes in coral hosts

212 and zooxanthellae. The gene sequences selected in the figure are more than 50%

213 similar to the corresponding gene sequences included in the KEGG database. The

214 phylogenetic tree was drawn by MEGA software, and the values indicate the branch
215 lengths. Gene ID indicates the ID number of the sequence in the transcriptome on the
216 comparison, beginning with TRINITY for host and SymbC1.scaffold for zooxanthellae.
217 Type indicates the specific type of the enzyme encoded by the genes, which was
218 obtained through the KEGG module, Pfam, and Swissprot databases. Species
219 indicate the similar species to which the sequence was compared in the NCBI-NR
220 database. Relative expression levels are the log_2fc values of each treatment group
221 compared to the control LS. P indicates the significance of the difference between
222 each treatment group and LS.

223 **Transcriptomic features of carbon metabolism of the coral host and**
224 **zooxanthellae**

225 To explore the underlying mechanisms of DIC accumulation and transportation of the
226 symbiotic system on a molecular level, we investigated the carbon-involved
227 metabolisms in different coral treatments.

228 Glycolysis (purple arrows in Fig. 4c) and gluconeogenesis (red arrows in Fig. 4c)
229 pathways were used as indicators for glucose utilization activities. In zooxanthellae,
230 compared to LS, all 9 genes annotated in glycolysis were down-regulated in DG, DS,
231 and LG, and the genes encoding three rate-limiting enzymes of glycolysis,
232 glucokinase (GLK) / hexokinase (HK), 6-phosphofructokinase (PFK),
233 and pyruvate kinase (PK)[35,36], were 2 out of 3 significantly down-regulated ($log_2fc > 1$,
234 $p < 0.05$) in DG. These lines of evidence pointed to external glucose being poorly
235 utilized by zooxanthellae, as was also evident from its DEGs of photosynthesis (Fig.

236 S2). Meanwhile, the genes encoding the rate-limiting enzymes of gluconeogenesis,
237 PEPCK2 and fructose-1,6-bisphosphatase (FBP)[37], were up-regulated in all three
238 treatments, even significantly up-regulated ($\log_2 fc > 1$, $p < 0.05$) in DG, suggesting
239 that it was consuming its own fatty acids to generate glucose. In contrast, in coral
240 hosts, out of 9 glycolysis-related DEGs, although 7 and 9 genes were down-regulated
241 in DG and DS, respectively, but 7 genes (including three rate-limiting genes) were
242 unchanged or up-regulated in the light group LG, which is in accordance with the
243 result from Fig. 2c-LG. Unsurprisingly, partial gluconeogenesis-related genes (e.g.,
244 PEPCK1) of the host were up-regulated in DG, DS and LG, probably due to the
245 external glucose decrease in the post-culture period.
246 The TCA cycle (brown arrows in Fig. 4c), which is the central pathway for CO_2
247 production in aerobic organisms, was further explored. In zooxanthellae, compared to
248 LS, the TCA cycle generally exhibited a decreased pattern, suggesting a deceleration
249 in respiration. Specifically, 9, 8 and 7 out of 13 genes annotated in the TCA cycle were
250 down-regulated in DG, DS, and LG, respectively. As to DEGs in coral hosts, almost all
251 genes were down-regulated in both dark treatment groups. Conversely, 10 out of 14
252 TCA-related genes were unchanged or up-regulated in LG, indicating that the host
253 accelerated respiration to produce CO_2 in the light, combined with the carbon
254 consumption in coral tissues from Fig. 2d-LG. This CO_2 was likely to be supplied to
255 the microalgae.

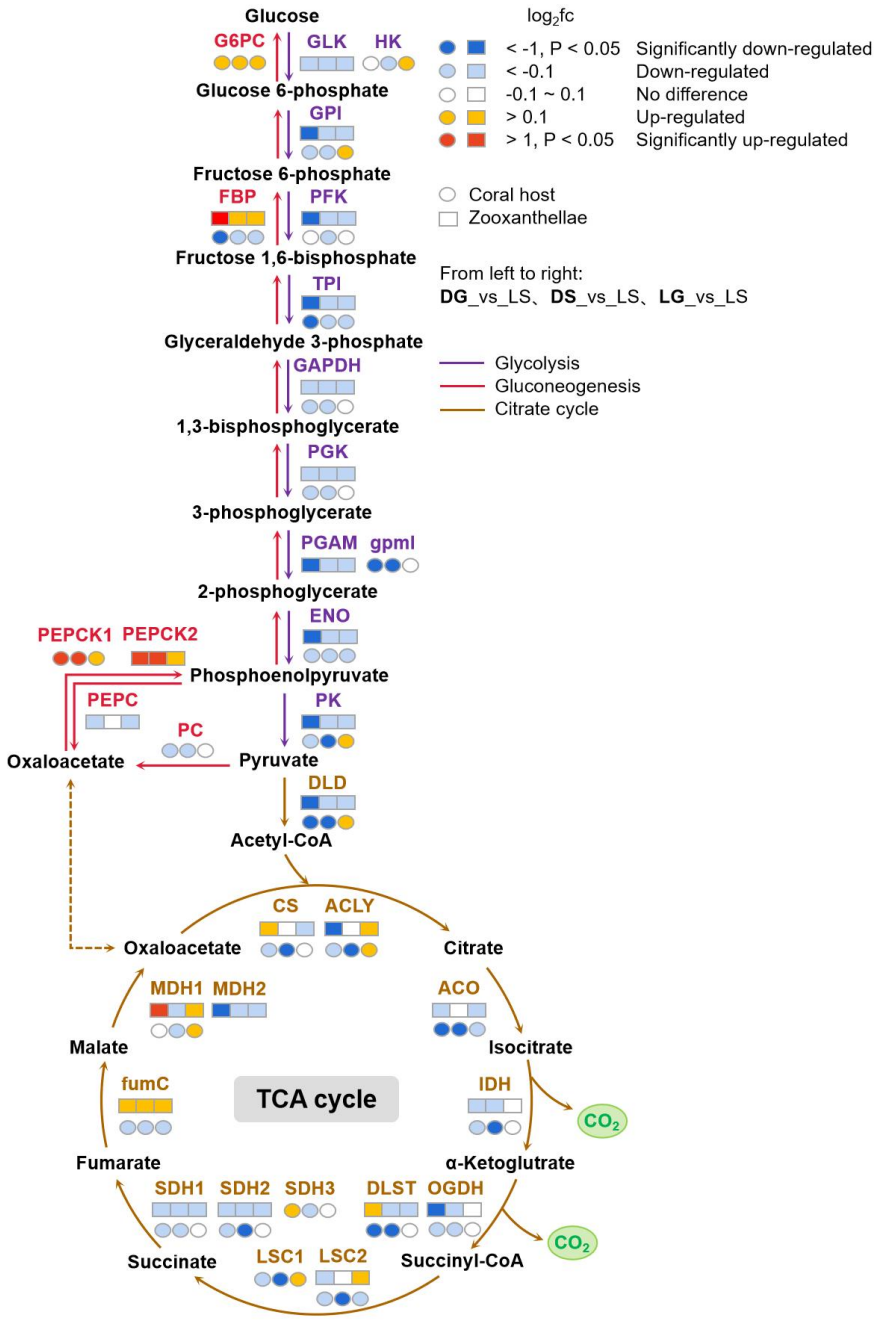

Fig. 4: DEGs of glycolysis, gluconeogenesis and TCA cycle genes in coral hosts and zooxanthellae. The expression results of one sequence with the largest length of the transcriptome compared with the reference sequence of the KEGG database were selected for each gene in the figure. ○ indicates coral host, and □ indicates zooxanthellae, where the colors indicate the log_2fc values of each treatment group compared to the control LS, from left to right once for DG, DS, and LG. Heatmap

263 colors indicate relative expression levels, also the log_2fc values of each treatment
264 group compared with the control LS. P indicates the significance of the difference
265 between each treatment group and LS.
266 Calcification, the coral-specific DIC metabolic pathway central to coral physiology
267 and health[38], was also analyzed. In general, calcification-related genes displayed a
268 decreased trend under dark conditions and an increased trend under light conditions.
269 Specifically, compared to the no-glucose added group (LS), out of the 88 ion
270 transporters DEGs responsible for active transportation, i.e., calmodulin (CaM),
271 calcium-binding proteins (CaBPs), Na^+/H^+ transports, HCO_3^- transports and CAs[39,40],
272 71 and 85 displayed a down-regulation in DG and DS, respectively (Fig. 5a), for a
273 total decrease of 59.31-log_2fc and 77.57-log_2fc (Fig. 5b). In contrast, the expression of
274 DEGs in LG was 58 out of 88 genes unchanged or up-regulated (Fig. 5a), for a total
275 increase of 20.05-log_2-fold (Fig. 5b), suggesting a correlation between coral
276 calcification and light, rather than glucose. Furthermore, galaxins, the sole skeletal
277 organic matrix proteins definitively identified in corals[41], continued to show a
278 consistent down-regulation in DG and DS, while exhibiting a 2.19-log_2-fold
279 up-regulation in LG (Fig. 5b). The DEGs of other skeletal organic matrix proteins
280 associated with early calcification, i.e., small cysteine-rich proteins (SCRiPs), orphan
281 taxonomically restricted genes (Orphan TRGs), coral acid-rich proteins (CARPs),
282 neurexins, and cartilage-related proteins[42,43,44,45], were over 90% down-regulated as
283 well in two dark treatments, but 50% unchanged or up-regulated in LG (Fig. 5a), which
284 provides further evidence of the predominant influence of light conditions, rather than

carbon sources on calcification.

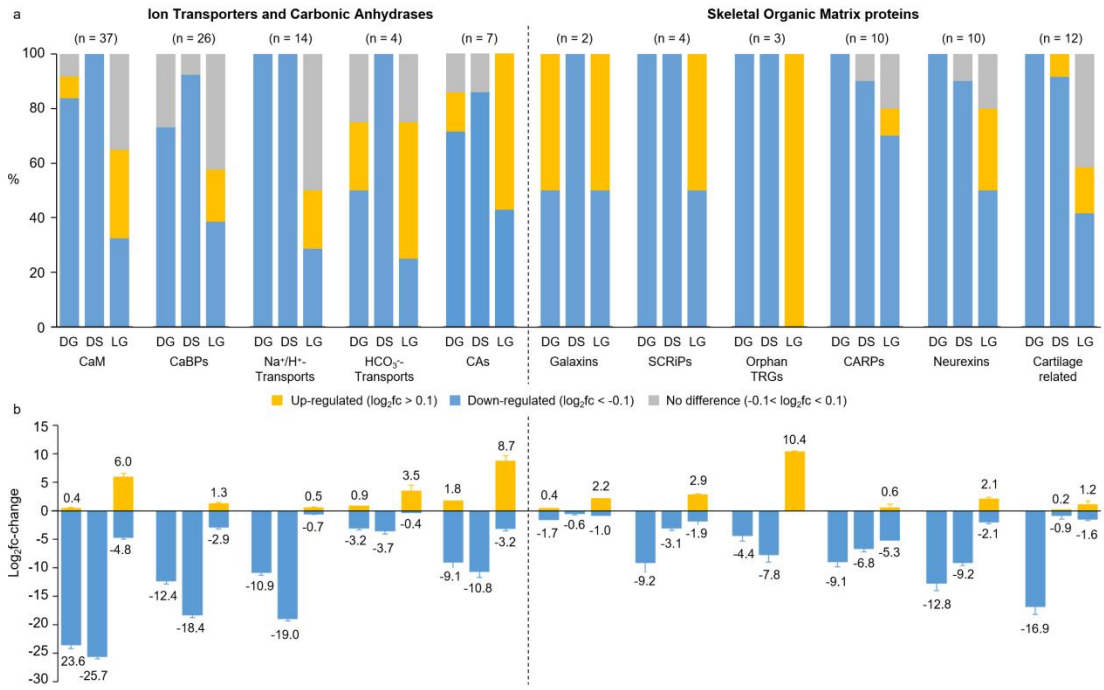

Fig. 5: Comparison of differential expression of genes related to calcification in coral hosts. a, Summary of changes on calcification genes in different categories (ion transporters, carbonic anhydrases, and skeletal organic matrix proteins) for DG, DS and LG treatments. Column colors indicate log_2fc values for each treatment group compared to control LS, with yellow up-regulated, blue down-regulated, and grey non-regulated. The total numbers of transcripts in each category are indicated above the corresponding bars. **b**, Summary of the corresponding mean log fold-change values for each of the classes of genes responding in part a. Actual fold-change values are indicated above or below each bar.

Elevated external CO_2 induced detachment of zooxanthellae

To examine our hypothesis that the coral may actively build a high concentration DIC pool inside for symbiont photosynthesis as a primary evolutionary strategy to “retain” symbiont microalga. Two scleractinian corals (*G. lobata* and *Acropora digitifera*) were

300 cultured at elevated CO_2 concentrations (1%) seawater. Results showed that
301 zooxanthellae would detach from the coral in the 1% CO_2 mixture gas supplied
302 seawater environments (Fig. 6a). At the same time, the corals maintained normal
303 zooxanthellae populations in the similar treatments with elevated CO_2 that contained
304 normal pH conditions (due to HCl addition), suggesting that higher CO_2 levels instead
305 of other factors play an decisive role in the loss of the corals' symbiotic algae. The
306 results of these experiments indicated that the chlorophyll of *G. lobata* and *A.*
307 *digitifera* decreased to about 50% of that in the control groups on day 12 and day 3 in
308 CO_2 supplied groups (Fig. 6b). We further explored whether the CO_2 solubility
309 impacted on the algae loss. In this study, the relationship between bubble diameter
310 and CO_2 solubility was determined by a Planktonscope and a total organic carbon
311 analyzer (Fig. S3abc). Results showed that smaller bubbles (d_{32} = 467 in group 2, Fig.
312 S3abc) in the microbubble plates led in higher CO_2 solubility (0.1703 g L^{-1} and 0.2000
313 g L^{-1} in group 2, Fig. 6c), and resulted in higher algal loss rates (59% and 84% in group
314 2, Fig. 6c). To determine whether stress impacted the coral bleaching, anti-oxidative
315 enzymes, i.e., superoxide dismutase (SODase) and catalase (CATase) activity were
316 detected. Compared to natural conditions, the CO_2 supplied treatments of two corals
317 were similar, but the HCl addition treatments significantly decreased the activities of
318 SODase and CATase (Fig. 6de, Two-way ANOVA, $p < 0.05$). Meanwhile, the
319 photosynthetic activity (Fv/Fm, Fig. S3d,e) of detached zooxanthellae in seawater
320 was similar to that of the symbiotic zooxanthellae and possessed higher CAs activity
321 (57.37 U g^{-1} $prot^{-1}$ and 46.32 U g^{-1} $prot^{-1}$, Fig. 6f) in two corals, suggesting that the

departure of zooxanthellae from the host was not caused by stress and they survived well outside of the corals.

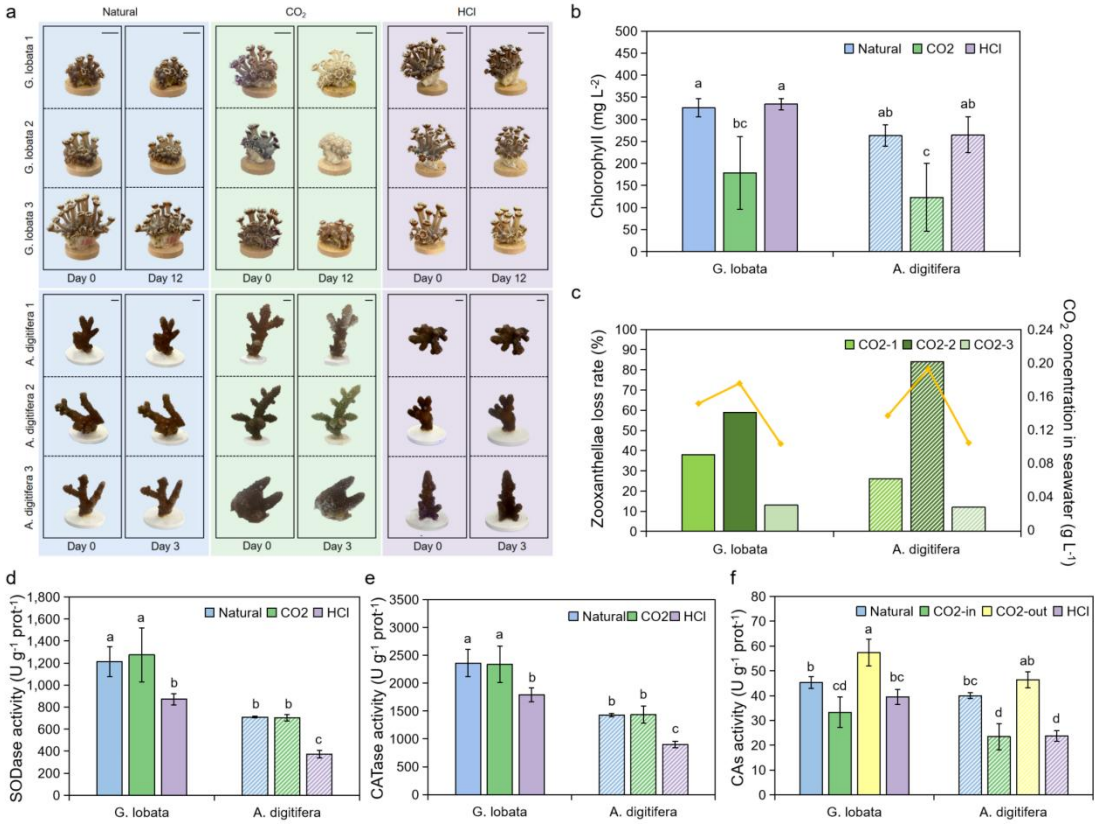

Fig. 6: Characterization of *G. lobata* and *A. digitifera* after external CO_2 and HCl addition. a, Morphological changes of corals. **b**, Chlorophyll of corals on the last day. **c**, Zooxanthellae loss rates (bar charts) and CO_2 concentration in seawater (line graphs) of three CO_2 treatments on the last day. **d**, SODase activity of corals on the last day. **e**, CATase activity of corals on the last day. **f**, CAs activity of corals on the last day. Natural indicates natural seawater control groups. CO_2 indicates 1% CO_2 mixture gas supplied treatments. HCl indicates pH reduction with HCl addition treatments. The graphs show the mean ± SD (n = 3). Letters above bars indicate a significant difference at $p < 0.05$.

Discussion

335 Coral reefs are highly productive ecosystems that thrive in oligotrophic waters. The
336 success of this Darwinian paradox is mainly attributed to the successful symbiotic
337 relationship between the coral host and the symbiont zooxanthellae[46,47]. Evidently,
338 efficient algal photosynthesis is paramount for this symbiotic system. However,
339 zooxanthellae possess type II Rubisco enzymes characterised by a low CO_2
340 affinity[14,15], and they have a relatively higher CO_2 demand, which consumes about
341 0.528 g CO_2 per gram of biomass grown (Fig. 1b). This is a far higher DIC demand
342 than that of other free living algae. For example, *Haematococcus pluvialis* consumes
343 0.308 g CO_2 for per gram of biomass growth[29], *Spirulina platensis* requires 0.256 g
344 CO_2[27], and *Chlorella vulgaris* requires requires 0.218 g CO_2[28]. Obviously, the
345 zooxanthellae are "high consumers" of DIC, implying the symbiont microalgae must
346 somehow cope with DIC limitation and perform photosynthesis successfully and
347 efficiently. It is reasonable that they may find high DIC sites or habitats within coral
348 tissue.
349 In this study, we found that the coral hosts are "high producers" of DIC and they can
350 continuously consume external organic carbon only in the presence of microalgal
351 photosynthesis in the light treatments (Fig. 2c-LG), whereas they cannot sustainably
352 utilize glucose (Fig. 2c-DG) and contract significantly (Fig. 2a-DG) in the dark. These
353 results indicated that the coral hosts were unable to eliminate their own produced CO_2
354 without symbiont photosynthesis. Surprisingly, we identified a high dosage DIC pool
355 within coral tissues independent of external environments, reaching up to 4.2 times
356 greater than external seawater under natural conditions (Fig. 2d-LS). This is

357 consistent with the findings obtained with dynamic modeling by Xu et al.[18]. We further
358 discovered that the DIC pool remained when no external DIC was provided (Fig.
359 2d-DG/LG), showing that it does not depend on external DIC concentrations. Why did
360 the coral hosts have a low DIC removal capacity, but accumulated a DIC pool? For
361 what purposes do the corals accumulate DIC? We hypothesize that the DIC pool
362 accumulated by corals may be the basis of the coral host-zooxanthellae symbiosis.
363 Since we know that the symbiont microalgae require high levels of DIC for
364 photosynthesis, the seemingly detrimental behaviour of accumulating DIC within coral
365 tissues would be beneficial or even necessary to the microalgal photosynthesis, which
366 in return would benefit the coral host by providing food continuously.
367 Results from the transcriptome support and explain our hypothesis on a molecular
368 level. Foremost, we found that the coral have evolved several DIC enriched pathways,
369 and they mainly serve the photosynthesis of the microalgae. Although several studies
370 have proposed that the host's CAs are involved in calcification[40,48], our results provide
371 evidence that the host CAs do not act primarily on their own calcification or emission
372 of respiration CO_2, because they have relatively low CAs activity in the dark compared
373 to the light (Fig. 3a). The CAs are most likely functioning to supply DIC to the algal
374 photosynthesis. This fully explains why coral hosts, having taken up enough DIC (Fig.
375 2d), continue to enrich their quantities of it. More detailed CA annotation results
376 indicate that coral host-symbiont may possess different CA types with distinct
377 functions and enhance carbon synergistically (Fig. 3d). Similarly, Tansik et al.[49] also
378 found that the supply of DIC in the coral symbionts is usually under the control of the

379 hosts. If that is true, there may have been other pathways that evolved to “retain” the
380 zooxanthellae during coral symbiosis that have not been discovered yet.
381 More interestingly, we have identified a potential carbon fixation pathway within coral
382 hosts that could supplement the CCMs, i.e., the PEPCK pathway. Notably, PEPCKase
383 can act as a carboxylase in invertebrates[50,51]. In natural conditions, when the
384 symbionts lacked DIC at the late stage, CAs activity gradually weakened while
385 PEPCKase activity gradually increased. At the same time, the gene expression of
386 three PEPCK sequences was significantly up-regulated (Fig. 3e-LS in red Gene ID),
387 which is different from the role played by PEPCK in gluconeogenesis (Fig. 3e-LS in
388 black Gene ID). In this process, PEPCKase may serve as PEPCase, converting PEP
389 into oxaloacetate, which efficiently concentrates DIC in the C_4 pathway, just as the
390 microalgal C_4 pathway has been reported[52,53,54]. There is another possibility that
391 oxaloacetate formation by PEPCKase replenishes the TCA cycle under increased
392 malate efflux, which accelerates tissue carbon flux to meet the photosynthetic
393 requirements of the microalgae. This mechanism bears similarities to the increasing
394 number of microalgal studies in recent years[55,56,57]. Notably, in the case of corals, the
395 hosts play a pivotal role in facilitating this step of carbon fixation for the symbiont.
396 Furthermore, CO_2 produced by host respiration is an important carbon source for
397 zooxanthellae photosynthesis. Under light conditions, the hosts’ glycolysis genes
398 (purple arrows in Fig. 4c-LG) and TCA cycle genes (brown arrows in Fig. 4c-LG) were
399 up-regulated, which showed that they were uptaking glucose to release CO_2. These
400 findings have similarities with previous studies that heterotrophic feeding and glucose

401 enrichment can elevate the respiration rate of coral hosts, subsequently enhancing
402 symbiont photosynthetic rates[58,59]. What's more, the hosts must prevent more CO_2
403 production without algal photosynthesis, i.e., by stopping the uptake of external
404 glucose and accelerating gluconeogenesis to meet its own metabolic needs (Fig.
405 4c-DG). All the above corroborate our physiological indicators (Fig. 2cde-DG, LG).
406 Surprisingly, our results suggest that coral calcification is more likely to be a provider
407 of DIC to microalgal photosynthesis rather than a competitor for DIC. Previous
408 experiments shown that calcification is a competitor for photosynthesis, consuming
409 60% of the respiration-based CO_2[19,20,21]. In contrast, it has been argued that there is
410 no competition, and calcification rates are higher under light conditions compared to
411 darkness[22,23,24]. Numerous hypotheses have been proposed to explain the
412 mechanisms behind light-enhanced calcification. The most widely supported
413 hypothesis suggests that the photosynthetic metabolites produced by algae can
414 supply ample nutrients for host growth, thereby accelerating the calcification
415 process[60,61,62]. However, in our experiment, even with sufficient external nutrition, all
416 coral calcification genes were down-regulated when exposed to darkness (Fig. 5-DG),
417 and up-regulated or unchanged in the light (Fig. 5-LG), suggesting that the correlation
418 between calcification and coral growth is not robust. This is consistent with
419 experimental results under dark conditions where both HCO_3^- in external seawater
420 and DIC in coral tissue remained utilized (Fig. 2b,d-DS), indicating that calcification
421 may not be an actively-driven process. It can be inferred that coral calcification
422 doesn't occur in tandem with host growth but is primarily fueled by the strong carbon

423 demands of symbiotic organisms. The CO_2 released during calcification isn't promptly
424 expelled from the coral body but is instead absorbed and utilized by zooxanthellae,
425 which may provide a new explanation for the controversial issue of the coral as a
426 carbon source or carbon sink[63,64].
427 Finally, to conclusively validate the significance of DIC in maintaining the health of this
428 symbiotic pair, we performed 1% CO_2 gas dosing addition experiments to increase the
429 DIC concentration by a factor of 1.2 times higher than the natural seawater. As
430 expected, two species of corals lost their zooxanthellae on day 3 and day 12,
431 respectively (Fig. 6ab), and interestingly the detached algae in seawater have higher
432 CAs activity (Fig. 6h) and similar photosynthetic efficiency (Fig. S3d,e) than those
433 within corals. This suggests that the coral bleaching in our experiments was not a
434 result of the coral host expelling zooxanthellae which not functioning properly, but
435 most likely a result of the algae actively departing from the coral. From an evolutionary
436 biology view, the algae's behavior is paradoxical, implying that they actively abandon
437 the protection of their hosts. However, our experiments dramatically increased CO_2
438 concentration in a short time, which could avoid the limitation of other nutrient factors
439 and make the algae respond more quickly. Notably, it was high CO_2 rather than low
440 pH that caused the algae to depart from the coral compared to the HCl addition
441 groups with the same pH. Meanwhile, the algal loss rates were positively correlated
442 with CO_2 solubility (Fig. 6b, c), suggesting that higher external CO_2 concentration was
443 more attractive to the algae. A study found a similar phenomenon that the increased
444 CO_2 caused stress and reduced zooxanthellae in *Galaxea fascicularis* and caused

445 bleaching[65]. This is good evidence explaining why coral hosts are desperately fixing
446 carbon because once the external DIC are sufficient for zooxanthellae growth, the
447 algal will no longer coexist in the host for “food”.
448 In summary, in this study, we provide a new perspective proposing that the coral host
449 actively accumulates DIC for the symbiont microalgae to understand the basis of coral
450 symbiosis. Coral hosts CCMs, respiration and calcification are all critical for the
451 accumulation of DIC for algal photosynthesis, and there are even other possible
452 carbon fixation pathways, i.e., PEPCK (Fig. S4). Furthermore, our hypothesis argues
453 that the coral bleaching caused by heatwaves and acidification[66,67,68] may not be
454 comprehensive, because it is also possible that as more greenhouse gases are
455 incorporated into the ocean, it results in a situation where the hosts can no longer
456 provide a relatively high CO_2 environment, and thus lose the attraction to the
457 microalgae, resulting in the collapse of the symbiosis. This may provide a new
458 perspective on coral bleaching under climate change. Undoubtedly, further
459 experimental efforts are needed to confirm these hypotheses.

460 **Methods**

461 **Coral collection**

462 The colonies of scleractinian corals (*G. lobata*) were collected in Dapeng Bay
463 (22°59’N, 114°33’E), Shenzhen, in September 2022. The coral colonies were
464 collected at a water depth of ~5 m and divided into 5×2×2 cm^3 blocks and then were
465 immediately transported to the indoor aquaria facilities of the Marine Biological
466 Laboratory (22°59’N, 113°97’E) at the Tsinghua Shenzhen International Graduate

467 School. Groups of 10 corals were cultured in 120 L aquariums filled with artificial
468 seawater (salinity = 33‰, pH = 8.2, T = 23-24 °C, light/dark = 12 h/12 h, Illumination
469 with blue-dominated coral lamps in natural light, light intensity = 20 μmol $m^{-2}s^{-1}$). After
470 allowing the corals to acclimatise to the laboratory environments for one month, we
471 initiated our experiments.

472 **Zooxanthellae isolation**

473 Zooxanthellae were first isolated from the host. Coral tentacles were clipped, and the
474 *Symbiodinium* sp. were blown out repeatedly with a pipette gun and then
475 resuspended in seawater. The algae pellet was centrifuged at 1000 g for 5 min at
476 20 °C. Subsequently, the remaining host debris was removed using differential
477 gradient centrifugation (900 g for 5 min → 700 g for 5 min → 650 g for 5 min at
478 20 °C)[69,70,71]. The final pellet was centrifuged at 2000 g for 10 min at 20 °C and
479 resuspended in F/2 medium, and then examined through an inverted microscope
480 (Primo Vert, Germany) at 40× magnification. Isolated zooxanthellae were enriched in
481 F/2 medium for further experiments.

482 **Zooxanthellae carbon demand measurement**

483 The carbon demand of zooxanthellae was evaluted following the description by Wu et
484 al.[29]. The seawater used in the experiment was decarbonised by the method of
485 Yellowlees et al.[72] and then added with corresponding concentrations of bicarbonate
486 ($NaHCO_3$). In detail, the pH was first adjusted to 4.5 with 1 M HCl to convert all DIC to
487 CO_2. Then, CO_2 was removed by simultaneous aeration with N_2 and agitation for 1 h.
488 1 mM Tris was then added, after which the pH was adjusted to 8.2 with 1 M of NaOH

489 to ensure the pH stability. Different amounts of $NaHCO_3$ were added to 40 mL-sealed
490 headspace bottles containing 20 mL of artificial seawater medium as a carbon source,
491 resulting in a final HCO_3^- concentration of 2 mM, 4 mM, and 8 mM, respectively. An
492 aliquot of 2 mL of zooxanthellae culture (about 5.6×10^6 cells mL^{-1}) was added to each
493 headspace bottle. Each dosage was triplicated independently. These experiments
494 were conducted with continuous illumination (blue light, 20 μmol $m^{-2}s^{-1}$) at 23-24 °C[73],
495 and pH was maintained at 8-8.5[74].
496 To ensure that DIC was the only variable and to exclude the effects of changes in
497 nitrogen and phosphorus concentrations and light on algal growth, the incubation
498 period was 36 h (Excluding other nutritional factors, i.e., N, P). To avoid CO_2 diffusion
499 to the air, the headspace bottles were sealed except during the sampling process, and
500 a control group with only 22 mL of the corresponding concentration of $NaHCO_3$ was
501 added at each treatment to serve as a blank for the changes of DIC concentrations.
502 The biomass and DIC concentration in solution were measured every 12 h. Cell
503 counts were performed with a hemocytometer under an inverted microscope (Primo
504 Vert, Germany). Cellular dry weight was calculated by drying the algae in an oven at
505 55 °C for more than 24 h to keep cell weight constant. The standard curve between
506 the cell counts and dry weight was established by preliminary experiments (Table. S2),
507 and the dry weight of the biomass in this experiment was estimated based on cell
508 counts. DIC concentrations were measured using a total organic carbon analyzer
509 (EC0075, Japan), which detects dissolved CO_2, HCO_3^-, and CO_3^{2-} in solution. The
510 average specific growth rate (g $L^{-1}d^{-1}$) over any two-time points was obtained by the

following equation:

$$\mu' = \frac{\ln N_2 - \ln N_1}{t_2 \quad t_1}$$

where N_2 and N_1 are the cell counts (g L^{-1}) at time t_2 and t_1, respectively.

Coral absorbance of organic and inorganic carbon under different light conditions

These experiments were carried out under two different light conditions: light (light/dark = 12 h/12 h, 20 μmol $m^{-2}s^{-1}$) and dark (continuous darkness), with or without organic carbon. Here, organic carbon is defined as decarbonised seawater with glucose (initial concentration of glucose 0.10 g L^{-1} based on the preliminary experiment) as the only carbon source, whereas inorganic carbon is defined as normal seawater with HCO_3^- (initial concentration of HCO_3^- 0.26 g L^{-1}) as the main carbon source.

In total, four experimental treatments were set: DG (Continuous darkness and glucose as the only carbon source), DS (Continuous darkness and $NaHCO_3$ as the only carbon source), LG (light/dark = 12 h/12 h and glucose as the only carbon source), and LS (light/dark = 12 h/12 h and $NaHCO_3$ as the only carbon source). Each coral was cultured independently in 1.6 L of the respective medium. To exclude possible interference from stored sugars, all corals used had been starved in darkness for 3 days before experiments. Triplicates of each treatment were conducted independently.

During the experiment, coral morphological changes were recorded every day using a camera at fixed points, and external DIC and glucose concentrations were detected

533 simultaneously. Whole coral tentacles were ground and homogenised, and then used
534 for measurements of carbon concentration and carbon fixation enzyme activities in
535 coral tissues every other day.

536 **Coral bleaching induction by CO_2 gas exposure**

537 Two different speciees of scleractinian corals (*G. lobata* and *A. digitifera*) were
538 selected for the coral bleaching experiment. The experiments were set up with three
539 treatments: CO_2 group (1% CO_2 mixture gas was continuously aerated into seawater
540 at 0.05 L min^{-1}, with the microbubble plates generating microbubbles with an average
541 size of 400-600 μm, pH = 7.0)，HCl group (1 M HCl was added to seawater daily to
542 adjust the same pH as the CO_2 group to examine the possible effect of changes pH on
543 the performance of coral, pH = 7.0) and control group (natural seawater, pH = 8.2),
544 and other conditions were kept the same (salinity = 33‰, T = 23-24 °C, light intensity
545 = 20 μmol $m^{-2}s^{-1}$, light/dark = 12 h/12 h). Each coral was placed in a 1.6 L system and
546 cultured independently. Each treatment was triplicated. During the experiment, the pH
547 of seawater and CO_2 solubility were measured daily. On the last day, free
548 zooxanthellae were collected from seawater, and symbiotic algae on corals were
549 separated with oral irrigation. Meanwhile, the symbiotic algae coverage,
550 photosynthetic activity (Fv/Fm), chlorophyll, carbon fixation enzymes, and
551 anti-oxidative enzymes' activities were detected. The dissolved CO_2 were measured
552 using a total organic carbon analyzer (EC0075, Japan), and its relationship with
553 microbubble diameter was determined with the Planktonscope image system (Oasis
554 Photobio Tech, China).

555 **Physiological parameters and enzymatic activities**

556 DIC concentration in seawater was measured using a total organic carbon analyzer
557 following the instruction manual (EC0075, Japan), and glucose concentrations were
558 measured by the dinitrosalicylic acid (DNS) method[75], DIC and glucose consumption
559 was calculated, respectively. A multi-excitation chlorophyll fluorometer was used to
560 measure the photosynthetic activity (Fv/Fm) of microalgal cells. ChlorophyII was
561 quantified using the methods of Ji et al.[76] and Laura et al.[77], respectively. Protein
562 concentrations were determined with the bicinchoninic acid (BCA) method[78] for
563 homogenisation of all assay metrics. The activities of carbon fixation enzymes, i.e.,
564 CAs, PEPCase and PEPCKase, and anti-oxidative enzymes, i.e., SODase and
565 CATase were measured by double antibody sandwich method using ELISA kits
566 (Thermo Fisher Scientific, USA).

567 **Transcriptomics analysis**

568 On day 8 of the coral culture experiments, all the corals were taken out and
569 fast-frozen with liquid nitrogen for transcriptomic analysis. Total RNA was extracted
570 using the Trizol-centrifugal column method, and then sent to the Shanghai Majorbio
571 Bio-pharm Technology Co., Ltd. (Shanghai, China) for the construction of an RNA-seq
572 transcriptome library. Each treatment was replicated three times. Raw reads were
573 trimmed and quality controlled by fastp (Version 0.19.5).

574 To distinguish the sequences of coral and zooxanthellae, the clean data from the
575 samples were used to do *de novo* assembly with Trinity (Version 2.8.5) initially, and all
576 the assembled sequencs were filtered by CD-Hit (Version 4.5.7) and TransRate

577 (Version 1.0.3) to increase quality. Species annotation was performed through the
578 NCBI-NR database to select coral species for subsequent analysis. Meanwhile, the
579 clean reads were aligned to reference genome of zooxanthellae (*Cladocopium*
580 *goreaui*, http://sampgr.org.cn/index.php/download) with orientation mode using
581 HISAT2 (Version 2.1.0), and the alignment rates ranged from 31.23% to 36.9%. The
582 mapped reads were assembled by StringTie (Version 2.1.2).
583 The expression level of each transcript was calculated according to the transcripts per
584 million reads (TPM) method. DEGs between four treatments were identified using
585 DESeq2 (Version 1.24.0), and DEGs with $|\log_2 FC| \geq 1$ and P-value < 0.05 were
586 considered to be significantly different expressed genes. Subsequently, DIAMOND
587 (Version 0.9.24) was used to compare with the NCBI-NR database for species
588 annotation, and with the KEGG database for functional annotation (E-value < 10^{-5},
589 identity ≥ 50%, and comparison length ≥ 50%). Metabolic pathways were mapped
590 using the KEGG Pathway as the primary reference. BLAST+ (Version 2.9.0) was used
591 to compare with KEGG, Swissprot, and Pfam databases to obtain more coding genes
592 and classification information of PEPC, PEPCK, and CA in the transcriptome.
593 **Statistical analysis and data availability**
594 All experiments were conducted with a minimum of three biological replicates to
595 ensure result reproducibility. The results are presented as mean ± standard deviation
596 (SD). Statistical analysis was performed using SPSS version 20.0 (SPSS Inc.,
597 Chicago, IL, USA). All data were analyzed using an unpaired Two-way ANOVA.
598 Statistical significance was determined at thresholds of 0.05. Genetic distances were

599 calculated using MEGA11 based on the P-distance model, and phylogenetic trees
600 were constructed using the Neighbor-Joining (NJ) method[79]. Heatmaps were drawn
601 using the pheatmap package in R (Version 4.2.3) and Z-Score normalisation was
602 performed.

603 **Data availability**

604 The data of this study are available within the article. Source data collected in this
605 study are available from Zenodo online (https://doi.org/10.5281/zenodo.11276136).
606 Raw RNAseq reads for differential gene expression analyses have been submitted to
607 NCBI's SRA database (http://www.ncbi.nlm.nih.gov) under BioProject PRJNA1115939.
608 The KEGG database (https://www.kegg.jp/) was used for functional enrichment
609 analyses.

610 **References**

611 1. Shi, T., Zheng, X. Q., Zhang, H., Wang, Q. F. & Zhong, X. Coral reefs: potential
612 blue carbon sinks for climate change mitigation. *Bull. Chin. Acad. Sci.* **36**,
613 270-278 (2021).

614 2. Webb, K. L., DuPaul, W. D., Wiebe, W., Sottile, W. & Johannes, R. E. Enewetak
615 (Enewetok) atoll: aspects of the nitrogen cycle on a coral reef. *Limnol. Oceanogr.*
616 **20**, 198-210 (1975).

617 3. Dobson, K. L. et al. Moderate nutrient concentrations are not detrimental to corals
618 under future ocean conditions. *Mar. Biol.* **168**, 98 (2021).

619 4. Wooldridge, S. A. A hypothesis linking sub-optimal seawater pCO_2 conditions for
620 cnidarian-*Symbiodinium* symbioses with the exceedence of the interglacial
621 threshold (>260 ppmv). *Biogeosciences* **9**, 1709-1723 (2012).

622 5. Muller-Parker, G., D'elia, C. F. & Cook, C. B. Interactions between corals and their
623 symbiotic algae. *Coral Reefs Anthropocene*, 99-116 (2015).

624 6. Wiedenmann, J. et al. Reef-building corals farm and feed on their photosynthetic
625 symbionts. *Nature* **620**, 1018-1024 (2023).

626 7. Titlyanov, E. & Titlyanova, T. Reef-building corals-symbiotic autotrophic
627 organisms: 1. general structure, feeding pattern, and light-dependent distribution
628 in the shelf. *Russ. J. Mar. Biol.* **28**, 1-15 (2002).

629 8. Rädecker, N., Pogoreutz, C., Voolstra, C. R., Wiedenmann, J. & Christian, W.
630 Nitrogen cycling in corals: the key to understanding holobiont functioning? *Trends*
631 *Microbiol.* **23**, 490-497 (2015).

632 9. Ferrier-Pagès, C., Godinot, C., D'angelo, C., Wiedenmann, J. & Grover, R.
633 Phosphorus metabolism of reef organisms with algal symbionts. *Ecol. Monogr.* **86**,
634 262-277 (2016).
635 10. Falkowski, P. G., Dubinsky, Z., Muscatine, L. & Porter, J. W. Light and the
636 bioenergetics of a symbiotic coral. *Bioscience* **34**, 705-709 (1984).
637 11. Treignier, C., Grover, R., Ferrier-Pagès, C. & Tolosa, I. Effect of light and feeding
638 on the fatty acid and sterol composition of zooxanthellae and host tissue isolated
639 from the scleractinian coral *Turbinaria reniformis*. *Limnol. Oceanogr.* **53**,
640 2702-2710 (2008).
641 12. Hayashida, H., Matear, R. J. & Strutton, P. G. Background nutrient concentration
642 determines phytoplankton bloom response to marine heatwaves. *Global Change*
643 *Biol.* **26**, 4800-4811 (2020).
644 13. Kumar, K. & Das, D. Carbon dioxide sequestration by biological processes.
645 In *Transformation and utilization of carbon dioxide*. Berlin, Heidelberg: Springer
646 Berlin Heidelberg. 303-334 (2014).
647 14. Whitney, S. M., Shaw, C. & Yellowlees, D. Evidence that some dinoflagellates
648 contain a ribulose-1, 5-bisphosphate carboxylase/oxygenase related to that of the
649 α-proteobacteria. *Proc. R. Soc. B* **259**, 271-275 (1995).
650 15. Raven, J. A., Suggett, D. J. & Giordano, M. Inorganic carbon concentrating
651 mechanisms in free-living and symbiotic dinoflagellates and chromerids. *J.*
652 *Phycol.* **56**, 1377-1397 (2020).
653 16. Xu, Y. et al. Coral symbiosis carbon flow: a numerical model study spanning

654 cellular to ecosystem levels. *Front. Mar. Sci.* **9**, 749921 (2022).

655 17. Al-horani, F. A., Al-mogherabib, S. M. & Beera, D. E. Microsensor study of
656 photosynthesis and calcification in the scleractinian coral, *Galaxea fascicularis*:
657 active internal carbon cycle. *J. Exp. Mar. Biol. Ecol.* **288**, 1-15 (2003).

658 18. Allison, N., Cohen, I., Finch, A. A., Erez, J. & Tudhope, A. W. Corals concentrate
659 dissolved inorganic carbon to facilitate calcification. *Nat. Commun.* **5**, 5741
660 (2014).

661 19. Goldberg, W. M. Coral skeletal chemistry: physiological and environmental
662 regulation of stable isotopes and trace eetals in *Montastrea annularis*. Proc. *R.*
663 *Soc. B* **196**, 1166-1173 (1977).

664 20. Langdon, C. & Atkinson, M. J. Effect of elevated pCO_2 on photosynthesis and
665 calcification of corals and interactions with seasonal change in
666 temperature/irradiance and nutrient enrichment. *J. Geophys. Res.* **110**, C09S07
667 (2005).

668 21. Uthicke, S. & Fabricius, K. E. Productivity gains do not compensate for reduced
669 calcification under near-future ocean acidification in the photosynthetic benthic
670 foraminifer species *Marginopora vertebralis*. *Glob. Change Biol.* **18**, 2781-2791
671 (2012).

672 22. Moya, A. et al. Carbonic anhydrase in the scleractinian coral *Stylophora pistillata*.
673 *J. Biol. Chem.* **283**, 25475 (2008).

674 23. Tambutte, S. et al. Coral biomineralization: from the gene to the environment. *J.*
675 *Exp. Mar. Biol. Ecol.* **408**, 58-78 (2011).

676 24. De Goeyse, S., Webb, A. E., Reichart, G. J. & De Nooijer, L. J. Carbonic
677 anhydrase is involved in calcification by the benthic foraminifer *Amphistegina*
678 *lessonii*. *Biogeosciences* **18**, 393-401 (2021).
679 25. Palardy, J. E., Grottoli, A. G. & Matthews, K. Effects of upwelling, depth,
680 morphology and polyp size on feeding in three species of *Panamanian* corals.
681 *Mar. Ecol. Prog. Ser.* **300**, 79-89 (2005).
682 26. Palardy, J. E., Rodrigues, L. J. & Grottoli, A. G. The importance of zooplankton to
683 the daily metabolic carbon requirements of healthy and bleached corals at two
684 depths. *J. Exp. Mar. Biol. Ecol.* **367**, 180-188 (2008).
685 27. Sydney, E. B. et al. Potential carbon dioxide fifixation by industrially important
686 microalgae. *Bioresour. Technol.* **101**, 5892-6 (2010).
687 28. Singh, S. P. & Singh, P. Effect of CO_2 concentration on algal growth: a review.
688 Renew. Sustain. *Energy Rev.* **38**,172-179 (2014).
689 29. Wu, K. et al. Optimizing the growth of *Haematococcus pluvialis* based on a novel
690 microbubble-driven photobioreactor. *Iscience* **24**, 103461 (2021).
691 30. Moroney, J. V., Bartlett, S. G. & Samulesson, G. Carbonic anhydrases in plants
692 and algae. *Plant Cell Environ.* **24**, 141-153 (2001).
693 31. Field, D., Tiwari, B. & Snape, J. Bioinformatics and data management support for
694 environmental genomics. *PLoS Biol.* **3**, 1352-1353 (2005).
695 32. Heyduk, K., Moreno-Villena, J. J., Gilman, I. S., Christin, P. A. & Edwards, E. J.
696 The genetics of convergent evolution: insights from plant photosynthesis. *Nat.*
697 *Rev. Genet.* **20**, 485-493 (2019).

698 33. O'Leary, B., Park, J. & Plaxton, W. C. The remarkable diversity of plant PEPC
699 (phosphoenolpyruvate carboxylase): recent insights into the physiological
700 functions and post-translational controls of non-photosynthetic PEPCs. *Biochem.*
701 *J.* **436**, 15-34 (2011).
702 34. Koendjbiharie, J. G., van Kranenburg, R. & Kengen, S. W. M. The
703 PEP-pyruvate-oxaloacetate node: variation at the heart of metabolism. *FEMS*
704 *Microbiol. Rev.* **45**, fuaa061 (2021).
705 35. Liu, Y. Q., Tang, S., Yan, Q., Zhou, J. & Cai, Z. H. Effectiveness and associated
706 mechanisms of a combination of biofilm attached cultivation and mixotrophy in
707 promoting microalgal biomass. *Bioresour. Technol.* **393**, 130077 (2024).
708 36. Windhagauer, M. et al. Metabolic response to a heterologous
709 poly-3-hydroxybutyrate (PHB) pathway in *Phaeodactylum tricornutum*. *Appl.*
710 *Microbiol. Biotechnol.* **108**, 1-16 (2024).
711 37. Legouis, D., Faivre, A., Cippà, P. E. & de Seigneux, S. Renal gluconeogenesis:
712 an underestimated role of the kidney in systemic glucose metabolism. *Nephrol.*
713 *Dial. Transplant.* **37**, 1417-1425 (2022).
714 38. Weis, V. M. & Allemand, D. What determines coral health? *Science* **324**,
715 1153-1155 (2009).
716 39. Tohse, H., Murayama, E., Ohira, T., Takagi, Y. & Nagasawa, H. Localization and
717 diurnal variations of carbonic anhydrase mRNA expression in the inner ear of the
718 rainbow trout *Oncorhynchus mykiss*. *Comp. Biochem. Physiol. Part B: Biochem.*
719 *Mol. Biol.* **145**, 257-264 (2006).

720 40. Allemand, D., Tambutté, É., Zoccola, D. & Tambutté, S. Coral calcification, cells to
721 reefs. *Coral Reefs: an Ecosystem in Transition*, 119-150 (2011).
722 41. Fukuda, I. et al. Molecular cloning of a cDNA encoding a soluble protein in the
723 coral exoskeleton. Biochem. *Biophys. Res. Commun.* **304**, 11-17 (2003).
724 42. Sunagawa, S., DeSalvo, M. K., Voolstra, C. R., Reyes-Bermudez, A. & Medina, M.
725 Identifification and gene expression analysis of a taxonomically restricted
726 cysteine-rich protein family in reef-building corals. *PLoS One* **4**, e4865 (2009).
727 43. Grasso, L. C. et al. The biology of coral metamorphosis: molecular responses of
728 larvae to inducers of settlement and metamorphosis. *Dev. Biol.* **353**, 411-419
729 (2011).
730 44. Mass, T. et al. Cloning and characterization of four novel coral acid-rich proteins
731 that precipitate carbonates in vitro. *Curr. Biol.* **23**, 1126-1131 (2013).
732 45. Wang, X. et al. The evolution of calcification in reef-building corals. *Mol. Biol. Evol.*
733 **38**, 3543-3555 (2021).
734 46. Goldberg, W. M. Coral food, feeding, nutrition, and secretion: a review. *Mar.*
735 *Organisms as Model Systems in Biology and Medicine*, 377-421 (2018).
736 47. Cui, G. et al. Molecular insights into the *Darwin paradox* of coral reefs from the
737 sea anemone *Aiptasia*. *Sci. Adv.* **9**, eadf7108 (2023).
738 48. Bertucci, A. et al. Carbonic anhydrases in anthozoan corals-a review. *Bioorg. Med.*
739 *Chem.* **21**, 1437-1450 (2013).
740 49. Tansik, A. L., Fitt, W. K. & Hopkinson, B. M. Inorganic carbon is scarce for
741 symbionts in scleractinian corals. *Limnol. Oceanogr.* **62**, 2045-2055 (2017).

742 50. Fukuda, W., Fukui, T., Atomi, H. & Imanaka T. First characterization of an
743 archaeal GTP-dependent phosphoenolpyruvate carboxykinase from the
744 hyperthermophilic archaeon *Thermococcus kodakaraensis* KOD1. *J. Bacteriol.*
745 **186**, 4620-4627 (2004).
746 51. Allemand, D. & Furla, P. How does an animal behave like a plant? Physiological
747 and molecular adaptations of zooxanthellae and their hosts to symbiosis. *C. R.*
748 *Biol.* **341**, 276-280 (2018).
749 52. Mamedov, T. G. & Chollet, R. Discovery of novel phosphoenolpyruvate
750 carboxylase (PEPC) genes and their active polypeptides in the green microalga
751 *Chlamydomonas reinhardtii*. *Proc. ANAS (Biol. Sci.)* **65**, 99-105 (2010).
752 53. Wu, S. et al. Proteomic and biochemical responses to different concentrations of
753 CO_2 suggest the existence of multiple carbon metabolism strategies in
754 *Phaeodactylum tricornutum*. *Biotechnol. Biofuels* **14**, 1-17 (2021).
755 54. Kupriyanova, E. V., Pronina, N. A. & Los, D. A. Adapting from low to high: an
756 update to CO_2-concentrating mechanisms of *Cyanobacteria* and microalgae.
757 *Plants* **12**, 1569 (2023).
758 55. Seo, S., Jeon, H., Chang, K. S. & Jin, E. S. Enhanced biomass production by
759 *Phaeodactylum tricornutum* overexpressing phosphoenolpyruvate carboxylase.
760 *Algal Res.* **31**, 489-496 (2018).
761 56. Wei, L. et al. Transcriptomic and proteomic responses to very low CO_2 suggest
762 multiple carbon concentrating mechanisms in *Nannochloropsis oceanica*.
763 *Biotechnol. Biofuels* **12**, 1-21 (2019).

764 57. Wang, Y. et al. Realization process of microalgal biorefinery: the optional
765 approach toward carbon net-zero emission. *Sci. Total Environ.* 165546 (2023).
766 58. Rädecker, N., Pogoreutz, C., Wild, C. & Voolstra, C. R. Stimulated respiration and
767 net photosynthesis in *Cassiopeia* sp. during glucose enrichment suggests in
768 hospite CO_2 limitation of algal endosymbionts. *Front. Mar. Sci.* **4**, 267 (2017).
769 59. Lyndby, N. H. et al. Effect of feeding and thermal stress on photosynthesis,
770 respiration and the carbon budget of the scleractinian coral *Pocillopora*
771 *damicornis*. *bioRxiv* 378059 (2018).
772 60. Gladfelter, E. H., Michel, G. & Sanfelici, A. Metabolic gradients along a branch of
773 the reef coral *Acropora palmata*. *Bull. Mater. Sci.* **44**, 1166-1173 (1989).
774 61. Colombo-Pallotta, M. F., Rodríguez-Román, A. & Iglesias-Prieto, R. Calcification
775 in bleached and unbleached *Montastraea faveolata*: evaluating the role of oxygen
776 and glycerol. *Coral Reefs* **29**, 899-907 (2010).
777 62. Bertucci, A., Forêt, S., Ball, E. E. & Miller, D. J. Transcriptomic differences
778 between day and night in *Acropora millepora* provide new insights into metabolite
779 exchange and light-enhanced calcification in corals. *Mol. Ecol.* **24**, 4489-4504
780 (2015).
781 63. Van der Heijden, L. H. & Kamenos, N. A. Calculating the global contribution of
782 coralline algae to carbon burial. *Biogeosciences* **12**, 7845-7877 (2015).
783 64. Van Dam, B. R. et al. Calcification-driven CO_2 emissions exceed "Blue Carbon"
784 sequestration in a carbonate seagrass meadow. *Sci. Adv.* **7**, eabj1372 (2021).
785 65. Hii, Y. S., Ambok Bolong, A. M., Yang, T. T. & Liew, H. C. Effect of elevated carbon

786 dioxide on two scleractinian corals: *Porites cylindrica* (Dana, 1846) and *Galaxea*
787 *fascicularis* (Linnaeus, 1767). *J. Mar. Sci*. 2009.
788 66. Heron, S. F., Maynard, J. A., van Hooidonk, R. & Eakin C. M. Warming trends and
789 bleaching stress of the world's coral reefs 1985-2012. *Sci. Rep.* **6**, 38402 (2016).
790 67. Hughes, T. P. et al. Global warming and recurrent mass bleaching of corals.
791 *Nature* **543**, 373-377 (2017).
792 68. Dove, S. G., Brown, K. T., Van Den Heuvel, A., Chai, A. & Hoegh-Guldberg, O.
793 Ocean warming and acidification uncouple calcification from calcifier biomass
794 which accelerates coral reef decline. *Commun. Earth Environ.* **1**, 55 (2020).
795 69. Treignier, C., Tolosa, I., Grover, R., Reynaud, S. & Ferrier-Pagé sa, C. Carbon
796 isotope composition of fatty acids and sterols in the scleractinian coral *Turbinaria*
797 *reniformis*: effect of light and feeding. Limnol. Oceanogr. **54**, 1933-1940 (2009).
798 70. Ferrier-Pages, C. et al. Summer autotrophy and winter heterotrophy in the
799 temperate symbiotic coral *Cladocora caespitosa*. *Limnol. Oceanogr.* **56**,
800 1429-1438 (2011).
801 71. Imbs, A. B., Yakovleva, I. M., Dautova, T. N., Bui, L. H. & Jones, P. Diversity of
802 fatty acid composition of symbiotic dinoflagellates in corals: evidence for the
803 transfer of host PUFAs to the symbionts. *Phytochemistry* **101**, 76-82 (2014).
804 72. Yellowlees, D. et al. Role of carbonic anhydrase in the supply of inorganic carbon
805 to the giant clam-zooxanthellate symbiosis. *Mar. Biol.* **115**, 605-611 (1993).
806 73. Gohari, M. Y. & Darki, B. Z. Physiological and biochemical responses of
807 dinoflagellate *Symbiodinium* sp. to the different light intensities. *Shahid Beheshti*

808 *Univ.* **4**, 524-533 (2020).

809 74. Søderberg, L. M. & Hansen, P. J. Growth limitation due to high pH and low
810 inorganic carbon concentrations in temperate species of the dinoflagellate genus
811 *Ceratium*. *Mar. Ecol. Prog. Ser.* **351**, 103-112 (2007).

812 75. Puspasari, F. et al. Characteristics of raw starch degrading α-amylase from
813 *Bacillus aquimaris* MKSC 6.2 associated with soft coral *Sinularia* sp. *Starch -*
814 *Stärke* **63**, 461-467 (2011).

815 76. Ji, M. K. et al. Biodegradation of bisphenol A by the freshwater microalgae
816 *Chlamydomonas mexicana* and *Chlorella vulgaris*. *Ecol. Eng.* **73**, 260-269
817 (2014).

818 77. Mydlarz, L. D. & Jacobs, R. S. An inducible release of reactive oxygen radicals in
819 four species of gorgonian corals. *Mar. Freshw. Behav. Physiol.* **39**, 143-152
820 (2006).

821 78. Rädecker, N. et al. Nutrient stress arrests tentacle growth in the coral model
822 *Aiptasia*. *Symbiosis* **78**, 61-64 (2019).

823 79. Koichiro, T., Glen, S. & Sudhir, K. MEGA11: molecular evolutionary genetics
824 analysis version 11. *Mol. Biol. Evol.* **7**, 3022-3027 (2021).

Acknowledgements

This work was supported by the Projects of Shenzhen Science and Technology Program（KCXFZ20211020163557022, KCXFZ20211020165547011), and the Cross Research and Innovation Funding of Tsinghua SIGS (JC2022004).

Author contributions

BY.Z. and ZH.C. conceptualised and designed the experiments. BY.Z., L.L., XM.T., YQ.L. and WM.X. performed the experiments. BY.Z., S.T. and JM.Z. analysed and visualised the data. BY.Z. and S.T. interpreted the results and wrote the manuscript. HS.B., J.Z., MC.B. and ZH.C. revised the manuscript.

Competing interests

The authors declare no competing interests.

836 **Supplementary information**

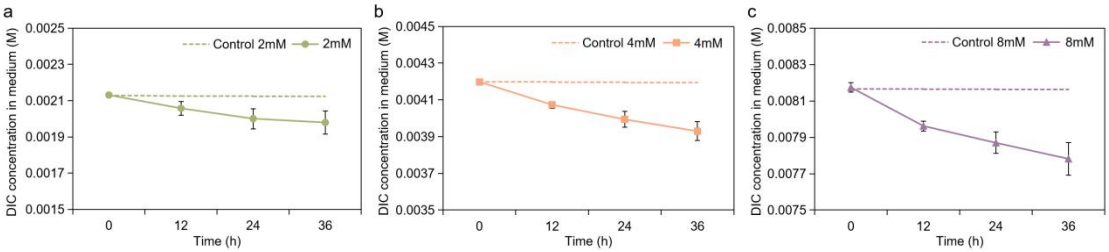

837

838 **Fig. S1: DIC consumption of monocultured zooxanthellae at different carbon**

839 **concentrations. a-c**, DIC concentration in medium at 2 mM, 4 mM and 8 mM

840 $NaHCO_3$ group. The graphs show the mean ± SD (n = 3).

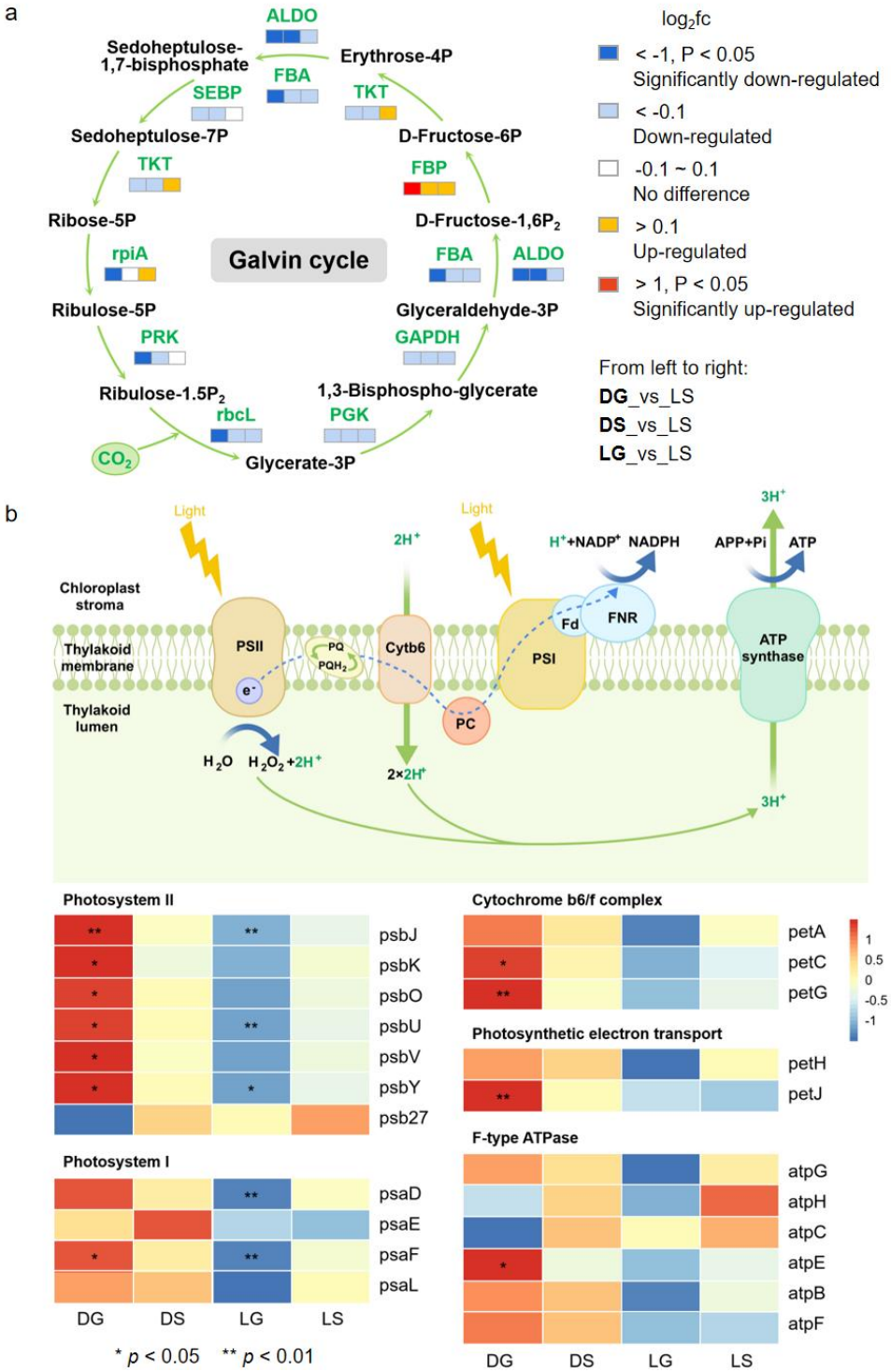

841

842 **Fig. S2: Comparison of the differential expression of photosynthesis genes in**

843 **zooxanthellae. a,** Carbon fixation genes in zooxanthellae. P_2 bisphosphate. P

844 phosphate. **b,** Photosynthesis photosystem genes in zooxanthellae. The expression

845 results of one sequence with the largest length of the transcriptome compared with

846 the reference sequence of KEGG database were selected for each gene in the figure.
847 The colors indicate the log_2fc values of each treatment group compared to the control
848 LS, from left to right once for DG, DS, and LG. Heatmap colors indicate relative
849 expression levels, also the log_2fc values of each treatment group compared with the
850 control LS. P indicates the significance of the difference between each treatment
851 group and LS.

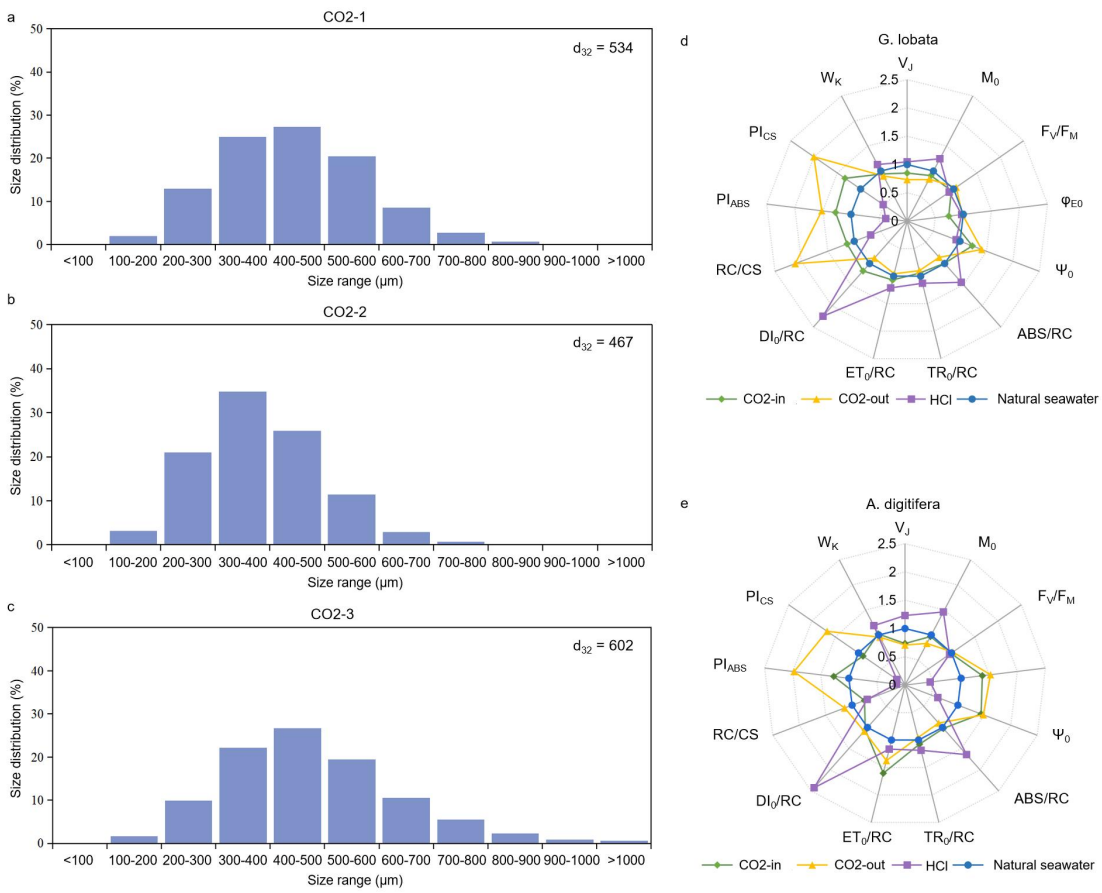

Fig. S3: Size range of microbubbles in CO_2 group and Chlorophyll fluorescence parameters of *G. lobata* and *A. digitifera*. a-c, Size range of microbubbles in CO_2 group 1-3. d_{32} indicate the diameters of microbubbles. **d-e**, Chlorophyll fluorescence parameters of *G. lobata* and *A. digitifera*, respectively. The related parameters used in chlorophyll fluorescence quantification were shown in Table. S1.

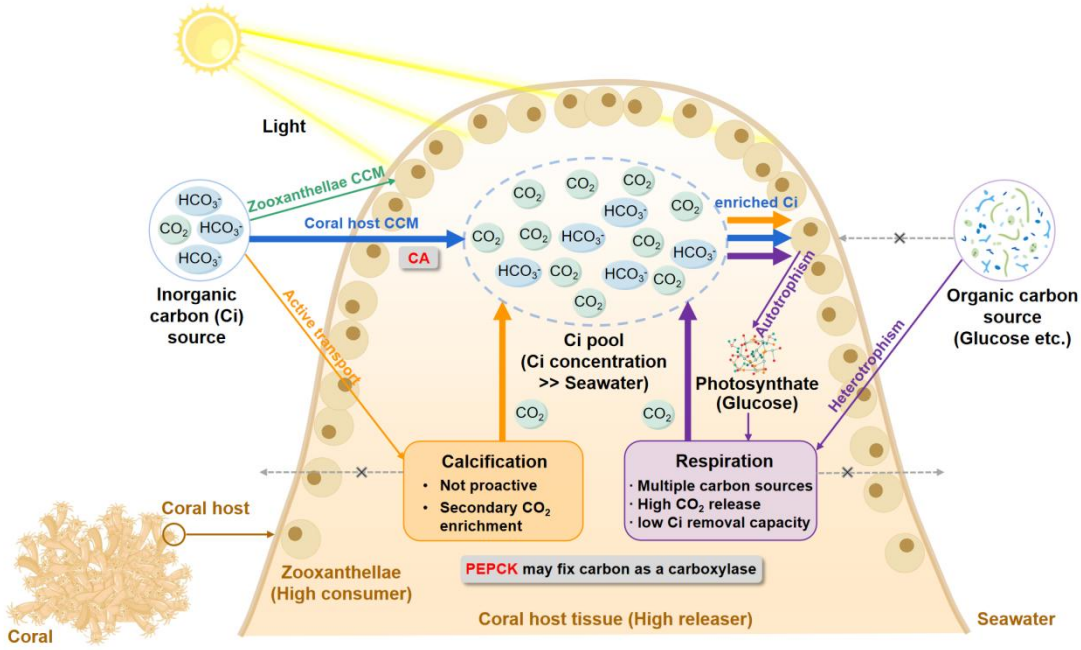

Fig. S4: Schematic diagram of the carbon fixation pattern of coral host-zooxanthellae symbiosis. The diagram indicates the internal tissue in one tentacle of the *G. lobata*. Arrow colors indicate different DIC pathways. Green indicates symbiotic algal CCM. Blue indicates host CCM. Yellow indicates host calcification. Purple indicates host respiration.

Parameters & Formula	Description
$V_J=(F_{2ms}-F_0) / (F_m-F_0)$	Relative variable fluorescence intensity at the J-step
$M_0=4(F_{300\mu s}-F_0) / (F_m-F_0)$	The rate at which QA is reduced
$F_V/F_m=1-(F_0/F_m)=\varphi_{p0}$	Maximum photochemical efficiency (at t=0)
$\varphi_{E0}=ET_0/ABS=[1-(F_0/F_m)]\ \Psi_0$	Quantum yield for electron transport (at t=0)
$\Psi_0=1-V_J$	Probability that a trapped exciton moves an electron into the electron transport chain beyond Q_A (at t=0)
$ABS/RC=M_0\ (1/V_J)\ (1/\varphi_{p0})$	Absorption flux per reaction center
$TR_0/RC=M_0\ (1/V_J)$	Trapped energy flux per reaction center for Q_A reduction (at t=0)
$ET_0/RC=M_0\ (1/V_J)\ \Psi_0$	Trapped energy flux per reaction center for electron transfer (at t=0)
$DI_0/RC=(ABS/RC)-(TR_0/RC)$	Dissipated energy flux per reaction center (at t=0)
$RC/CS=\varphi_{p0}\ (V_J/M_0)\ ABS/CS_0$	Density of per excited cross section
$PI_{ABS}=(RC/ABS)\ [\varphi_{p0}/(1-\varphi_{p0})]\ [\Psi_0/(1-\Psi_0)]$	Performance index based on absorbed light energy
$PI_{CS}=(RC/CS)\ [\varphi_{p0}/(1-\varphi_{p0})]\ [\Psi_0/(1-\Psi_0)]$	Performance index of light cross-section
$W_K=(F_k-F_0)/(F_J-F_0)$	The damage degree to the photosynthetic system

Table. S1: The related parameters, formula and related-descriptions used in chlorophyll fluorescence quantification.

	Group 1	Group 2	Group 3	Group 4	Group 5
Dry weight ($g\ mL^{-1}$)	0.0031	0.0032	0.0029	0.0031	0.0032
Cell counts ($cell\ mL^{-1}$)	7.64×10^{6}	7.80×10^{6}	7.50×10^{6}	7.60×10^{6}	7.68×10^{6}
Dry weight of individual cells ($g\ cell^{-1}$)	4.06×10^{-10}	4.10×10^{-10}	3.87×10^{-10}	4.08×10^{-10}	4.17×10^{-10}

867 **Table. S2: Preliminary experiments to calculate the standard curve between the**

868 **cell counts and dry weight of zooxanthellae.** Average = 4.05×10^{-10}, SD = 1.12

869 $\times 10^{-11}$.